Desalination and Water Treatment
www.deswater.com

doi: 10.5004/dwt.2020.26159

202 (2020) 112–120
October

Experimental and economic analysis of a permeate gap solar-driven membrane distillation system

S. Mejbri[a], K. Zhani[b,a,*]

[a]*Laboratory of Electromechanical Systems (LASEM), National Engineering School of Sfax, University of Sfax, 3038 Sfax, Tunisia*
[b]*Department of Mechanical, College of Engineering, University of Bisha, Bisha 61922, P.O. Box: 199, Saudi Arabia, email: kzhani@ub.edu.sa (K. Zhani)*

Received 7 December 2019; Accepted 23 May 2020

ABSTRACT

Remote areas are characterized by a lack of conventional energy sources, skilled personnel and maintenance facilities. Therefore, developing small-to-medium-size, stand-alone and robust solar desalination systems is necessary to provide freshwater independently in remote areas. This paper focuses on experimental studies of compact membrane distillation solar desalination prototype located at the Mechanical Engineering Department site of Kairouan University, Kairouan, Tunisia. The manufactured pilot system is totally autonomous. The electrical energy required to operate the unit is generated through a field of 4 m^2 of photovoltaic panels, and the heating of feedwater is provided by a field of 6 m^2 of solar collectors. The Kairouan plant performance of the first few months of operation is presented. The highest freshwater production of 148 L d^{-1} is obtained on a sunny summer day in July of 633 W m^{-2} d^{-1}. The economic analysis showed an impressive payback period and water production cost.

Keywords: Solar desalination; Membrane distillation; Experimental study; Economic analysis

1. Introduction

Water has long been thought of as a free and inexhaustible natural resource. Prospecting studies, however, reveal an alarming decline in water reserves at the scale of a quarter of a century, or even a decade. As typical for countries in the Middle East and North Africa (MENA) region, Tunisia is currently experiencing the crucial problem of supplying the public, agricultural and industrial water, particularly in the remote regions. Therefore, interest in desalination of the sea- and brackish water is rising. Today, in Tunisia, about 200.000 m^3 d^{-1} of freshwater is already produced by desalination. Globally, this is about 67 mio m^3 d^{-1}. Even if seawater is considered an unlimited source, the production of freshwater by conventional desalination systems like a multi-stage flash, multi-effect distillation, reverse osmosis, vapor compression, etc. is limited and quite expensive due to the high energy demand of the process. Another feature typical for countries in the MENA region is a very high gain of solar radiation: For Tunisia, this lies in the range of 2,000 kWh m^{-2} y^{-1}. Therefore, the use of solar energy for desalination is a logical step to securing an independent freshwater supply and minimizing the environmental impact due to CO_2 emissions. The use of solar-driven desalination plants can be an economically and technically preferable solution for small-scale and, in particular, decentralized applications. Besides the need for seawater desalination in Tunisia, there are many places in the countryside where the aquifer has an increasing salt content due to excessive deep welling, seawater intrusion or other geological reasons. In these rural areas, small- and medium-size desalination units, ranging between a couple of hundreds of liters per day to a couple of hundreds of cubic meters per day, are typically necessary to produce freshwater from the salty well water.

* Corresponding author.

At present, membrane distillation techniques are among the most promising methods. Their advantages over other processes of desalination are presented here [1,2]. The membrane distillation process (MD) was already studied and its potential interest, in the direct desalination of either the seawater that was demonstrated in the laboratory scale or the brackish water, was proved by several pilot-plants implanted in several regions such as North Africa and the Middle East. The membrane distillation, as its name indicates, involves a hybrid process combining at the same time the process of distillation and a process with the microporous hydrophobic membrane as a support for the interface liquid/vapor. The strength of transfer of the process is the transmembrane difference of partial pressure, which provokes the evaporation of the water in touch with the membrane. Salts stay in the solution and the diffuse steam through the pores of the membrane and then get back on the other side.

MD is an emerging technology. As its name implies, it is a hybrid process combining both the distillation and membrane processes. MD is mainly used for the treatment of aqueous feed solutions. It involves non-isothermal water transport in the vapor phase across a highly porous hydrophobic membrane that separates two aqueous solutions kept at different temperatures. The hydrophobicity of the membrane prevents the liquid phase penetrating the pores because of the surface tension although the membrane pores are larger than the single molecules. Hence liquid–vapor interfaces are created on either side of the membrane pores as shown in Fig. 1a. A driving force caused by the vapor pressure difference motivated by the difference in temperature between the feed side and the permeate one of the membranes [3–5] forces vapor molecules to pass the porous membrane structure. This phenomenon, also known as capillary depression, is shown in Fig. 1b. There are five possible configurations of membrane distillation (Fig. 2): direct contact membrane distillation (DCMD), permeate gap membrane distillation (PGMD), air gap membrane distillation (AGMD), sweeping gas membrane distillation (SGMD), and vacuum membrane distillation.

Few demonstration plants based on solar thermal membrane distillation technology for producing freshwater in remote areas have been mounted and tested worldwide. Recently, Andrés-Mañas et al. [7] developed and evaluated the performance of an innovative solar desalination system based on vacuum multi-effect membrane distillation

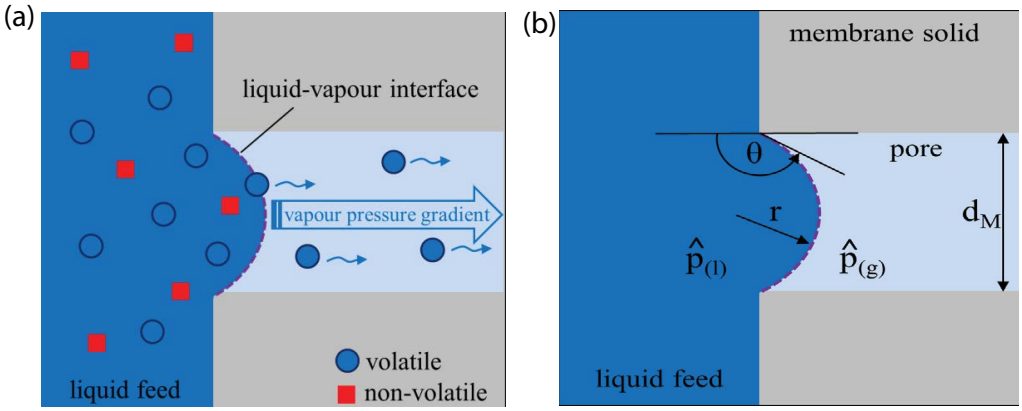

Fig. 1. Basic functional phenomena of the membrane distillation process [6]. (a) Evaporation at liquid-vapor interface and (b) capillary depression.

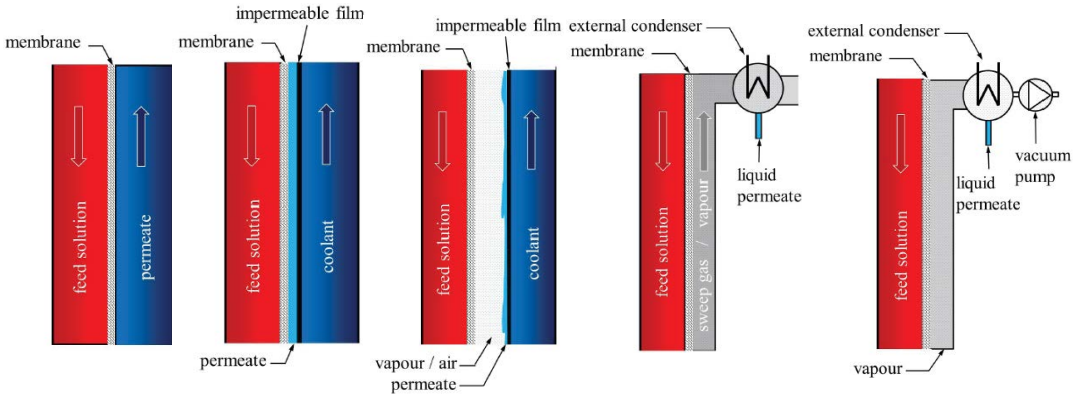

Fig. 2. Basic configurations of membrane distillation.

modules (V-MEMD) for the desalination of seawater at a pilot scale. The system was developed with three major components: the seawater intake, the solar collection field with a total aperture area of 35.9 m^2, and the MD device called MDS-40B of an effective area of 6.4 m^2. They highlighted that the optimal performance of the pilot system was obtained using a feed flow rate of 150 L h^{-1} and a hot feed temperature of 75°C. The highest distillate flux was 8.5 L h^{-1} m^{-2}, with a gain output ratio (GOR) of 3.19, and a recovery ratio of 36%; specific thermal energy consumption was around 200 kWh m^{-3}.

Kabeel et al. [8] conducted an experimental study on a pilot unit located at the University of Tanta, Tanta, Egypt. The studied system includes a direct contact membrane module and an evacuated tube water solar collector supported by an evaporative water cooler. Experimental results show that the system efficiency is more influenced by increasing water mass flow rate that the air one and reaches about 49.01%. The GOR of the system is 0.49. It was also found that cooling water flow rate impacts water extraction, however, freshwater production diminishes with rising cooling water temperature and attains its maximum value of 33.55 and 26.76 L d^{-1} respectively with and without cooling unit at the same operating conditions.

Chafidz et al. [9] demonstrated the performance of a portable hybrid solar-powered membrane distillation system installed on the rooftop of the engineering college building at King Saud University, Riyadh, Saudi Arabia. The apparatus, which was portable in design, had five major components: thermal storage tank, heat exchanger, evacuated tube thermal collectors, and V-MEMD made by Memsys (Germany). The results of the experiment as presented by the authors revealed a total volume distillate output of approximately 70 L and conductivity of approximately 4.7 μS cm^{-1}.

Fath et al. [10,11] experimentally studied the thermal performance of a stand-alone membrane distillation system under the climatic conditions of Alexandria, Egypt. According to their experimental results, without heat storage, the system can produce 11.2 L m^{-2} d^{-1} using 7.25 kWh m^{-2} d^{-1} of total solar energy. Fath et al. [10] reported that the plant demonstrated a high salt rejection rate as it decreased the electric conductivity of the feed water from 670 to about 3 μS cm^{-1}.

At the campus of the University of Science and Technology (JUST) in Jordan, Banat et al. [12] presented a 120 L d^{-1} autonomous solar desalination system called "compact SMADES" with a distillate conductivity of approximately 5 μS cm^{-1}. Their system, which was tested in Irbid, consisted of four main equipment pieces: a 5.73 m^2 flat solar thermal collector, the photovoltaic panel, a 475 L feed tank and a 10 m^2 spiral-wound AGMD. The membrane distillation module used in their experiments was developed and manufactured by Fraunhofer Institute for Solar Energy Systems (Germany) with the following characteristics: polytetrafluoroethylene, 0.2 μm pore diameters, 35 μm thickness and 80% porosity. They reported that the distillate flux reached 19 L d^{-1} m^{-2} ap. area for about 7 kWh m^{-2} of daily irradiation of. This value is around 4 times the daily production rate of conventional solar stills. It was found that the GOR of the used module was between 0.3 and 0.9 and the efficiency of the solar collector was about 45%. Banat et al. [13] continued to test another solar desalination system called "large SMADES" located at the Marine Science Station of Aqaba in Jordan. The system was meant to enhance the performance of the previous "compact SMADES". The main improvements are to (i) integrate a thermal storage tank of 3 m^3 and a battery bank to store thermal and electrical energy for additional operating hours after sunset; (ii) separate the collector area loop of 72 m^2 from the seawater loop of the MD module (two-loop system), which made the use of anti-corrosive material redundant; and (iii) couple four MD modules in parallel with an effective membrane area of 10 m^2 in each of module. From the results, the output from the unit was between 2 and 11 L d^{-1} m^{-2} ap. the area with specific energy consumption between 200 and 300 kWh m^{-3}.

As reported in membrane literature, the PGMD is the least studied MD configuration compared to DCMD, AGMD, and SGMD. The present work aimed to experimentally study the functioning of a solar desalination system coupling a field of flat plate solar collectors and a spiral wound PGMD. The pilot system was built in Kairouan, a city in the middle of Tunisia, with an average daily solar radiation of 8 kWh d^{-1}. The system was tested and assessed to gain comprehensive knowledge about the interaction of solar heat supply, performance of membrane and quality of drinking water.

2. Methods

2.1. Experimental set-up and instrumentation

In this section, the experimental set-up of PGMD and its instrumentation are described. Figs. 3 and 4 show the front and rear view photographs of the solar membrane distillation pilot system, respectively. The thermally driven desalination pilot system, based on the principle of MD, is designed, constructed and installed at Kairouan University for research purposes and laboratory operations. As shown in Fig. 5, the MD unit can be subdivided into four hydraulic circuits the solar energy circuit, including water solar collectors; the desalination circuit, including the MD module, a cartridge filter (F.001), the feed pump (P.001), the feed tank (S.001) and the flow indicator (F.001); the refilling circuit, including the refilling pump (P.002) and a cartridge filter; the distillate circuit, including the distillate tank (S.003) and the distillate pump (P.003). To protect water solar collectors from scaling and corrosion, the solar energy circuit is a hydraulically closed loop and is separated from the desalination circuit by a heat exchanger. The heat exchanger is operated with solar thermal collectors external heat supply for heating the hot feed water stream. For the cooling of the cold feedwater stream, no heat exchanger is included. The cooling can be provided over the intake of cold feedwater. The electrical energy demand of the pilot system is also supplied externally by photovoltaic panels. The operating principle of the current pilot system is as follows. Feedwater from the feed water tank (S.001) is pumped by the feed pump (P.001) into the MD-module (M) at the condenser inlet (C_in). In the condenser channel, the temperature of the feedwater will be increased before it enters the heat exchanger for further temperature increase. Afterward, it

Fig. 3. Front view of the solar-membrane distillation pilot system.

Fig. 4. Rear view of the solar membrane distillation pilot system.

again enters the MD-module at the evaporator inlet (E_in). Here, a part of the water evaporates and the vapor permeates through the membrane. On the opposite side, the vapor condenses and liquid distillate is formed in the distillate channel. The distillate and the brine exit the MD-module. The brine is recirculated to the feed tank while the product water is collected in the distillate tank (S.002). The distillate tank is fitted with a small submerged pump that can be triggered by the control system to extract the distillate from the tank at a set-point level value. The current experimental setup is equipped with several types of sensors listed in Table 1 and with an Agilent 34972A data acquisition system that contains a three-slot mainframe with a built-in 6 1/2-digit digital multimeter connected to a Personal Computer for central control and storage of the data. A list of sensors used to control and determine, respectively, the input and output process parameters involved in the experimental set-up, including the name of the component in the schematic of Fig. 5 and its accuracy, is presented in Table 1.

2.2. *Uncertainty analysis*

The uncertainty in the experimental results presented in this work is estimated using the approach described by

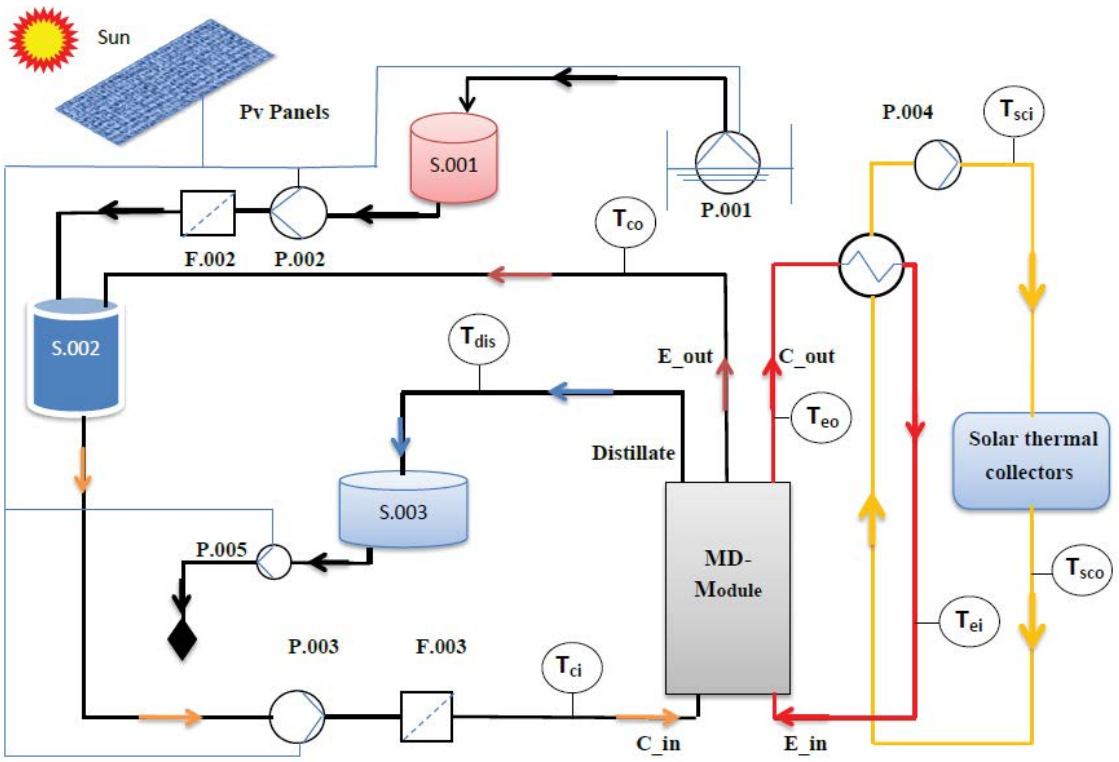

Fig. 5. Flow diagram of the MD Kairouan compact system.

Table 1
List of actors and sensors of the pilot system

Component	Producer	Type	Accuracy	Name in schematic
Temperature sensors	TSERI (Cyprus)	Thermocouple Type J	–50°C and +400°C	Tsci.Tsce.Tei.Tes.Tci.Tce. Tdist
Pyranometer	Delta OHM (Italy)	LP LYPRA 03AC	0–2,000 W m^{-2} 4.20 mA	–
Feed pump	Shurflo (USA)	LS2255	–	P.003
Filling pump	Shurflo	LS2255	–	P.002
Feed volume flow	LZS (India)	60/185 (2/96)	H_2O with 20°C 0.600L h^{-1}	–
PLC (Programmable logic controller)	Agilent Technologies (USA)	Data Logger 3 Agilent 34972A	–	–

Barford [14] and Moffat [15]. The uncertainty in the measurements is defined as the root sum square of the fixed error of the instrumentation and the random error observed during different measurements. The systematic experimental error for temperature is ±0.5°C and the solar radiation is ±5 W m^{-2}.

3. Results and discussion

The fabricated and installed solar desalination membrane prototype was put under experimentation over five months (from July to November 2018) to evaluate its thermal performance. Experimental measurements were taken on the solar collector's field and the PGMD module. The experiments were carried out under the climatic conditions of Kairouan, Tunisia. Every 1 min for up to 9 h, the measurements of all the parameters studied were taken and recorded. The measured climatic conditions of solar radiation and ambient temperature for a clear day characterized by high solar radiation in July are presented in Fig. 6. It can be seen that solar irradiation reaches its maximum value at about 900 W m^{-2} at noon and ambient temperature varied around 40°C. Results presented in Figs. 7 and 8 refer to these climatic conditions. Fig. 7 shows that inlet and outlet temperatures of the solar collector follow a similar trend as solar radiation. At noon, for a feedwater flow rate of 0.167 kg s^{-1} and an inlet water temperature of 50°C, the outlet water temperature reaches its maximum value at about 80°C. Fig. 8 presents that the temperatures are low in the early morning, reach their maximum at noon and go down towards the end of the afternoon. At the evaporator, channel temperatures gradually decrease from inlet to outlet, and on the contrary

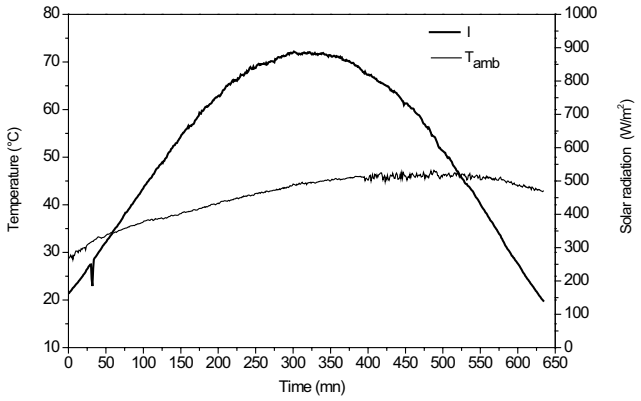

Fig. 6. Climatic conditions measured during a typical clear summer day in July (date: 25/07/2018).

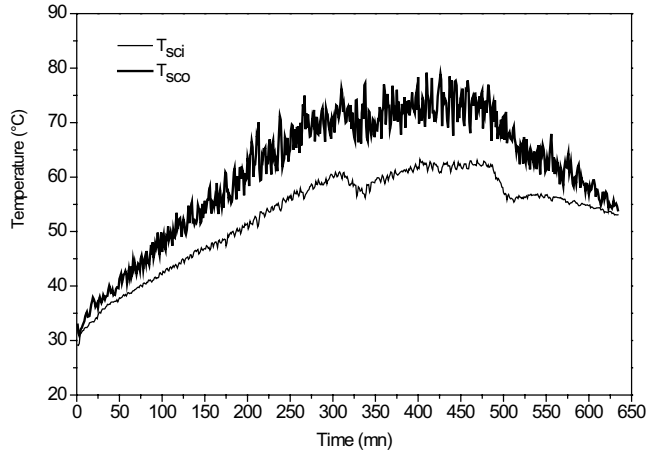

Fig. 7. Solar collector field dynamic behavior during experiments on a clear summer day (date: 25/07/2018).

at the condensation channel, temperatures increase from the inlet to the outlet. It can also be observed that the temperature of the distillate and at the inlet of the condenser channel are very close, which reflects the effectiveness of the heat transfer process inside the PGMD module.

Figs. 9 and 10 depict the dynamic behavior of input and output temperatures of the MD system during experiments on two consecutive fall days characterized by high fluctuations of solar intensity. It can be noticed that the solar collector and PGMD module have a good response time to the solar radiation fluctuations. Fig. 10 shows the highest recorded solar radiation of 1,000 W m^{-2}, and the correspondent daily production is of 118 L d^{-1}.

The influence of the variation of feed water volume flow on distillate is shown in Fig. 11. Two tests were conducted for ten different days during July 2018. For each test, we varied the feed water volume flow from 200 to 600 L h^{-1} for five different days. Fig. 11 shows that, for the two tests, the distillate increased with the feed flow. As is evident from Fig. 11, distillate values obtained in test 2 are higher than those in test 1 and the highest value achieved is 148 kg d^{-1}. The maximum distillate value is obtained for the climatic

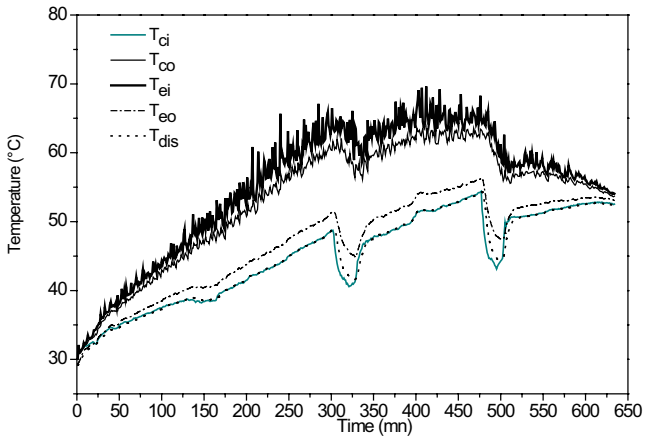

Fig. 8. PGMD module dynamic behavior during experiments on a clear summer day (date: 25/07/2018).

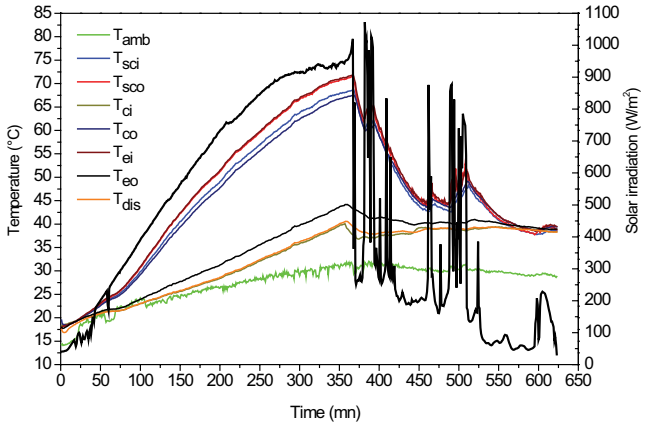

Fig. 9. MD system dynamic behavior during experiments on a cloudy fall day (date: 05/10/2018).

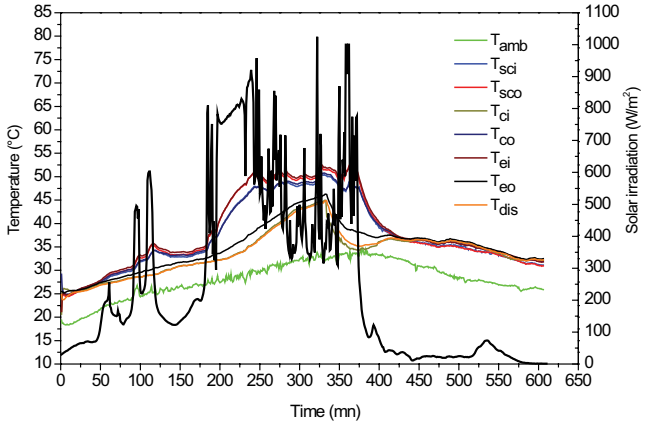

Fig. 10. MD system dynamic behavior during experiments on a cloudy fall day (date: 06/10/2018).

and operating parameters shown in the row highlighted in Table 2, which is characterized by high solar radiation, 633 W m^{-2}, and high feed volume flow 0.167 kg s^{-1}. The reason the distillate increases with increasing feed

Table 2
Experimental average values of the main parameters in the PGMD module

Days	I (W m^{-2})	T_{amb} (°C)	$\dot{m}_{feed}$ (kg s^{-1})	T_{sco} (°C)	T_{co} (°C)	T_{ei} (°C)	T_{eo} (°C)	T_{dis} (°C)	$\dot{m}_{dis}$ (kg d^{-1})
20/07/2018	591	40.108	0.056	58.993	50.491	50.528	42.820	41.532	43
21/07/2018	634	44.244	0.083	64.363	53.552	55.231	46.121	44.923	70
23/07/2018	544	36.532	0.111	52.413	49.384	51.568	41.461	39.680	97
24/07/2018	664	36.032	0.139	57.299	54.244	56.595	46.869	44.854	144
25/07/2018	633	40.640	0.167	55.286	53.038	55.549	45.709	43.669	148
04/10/2018	399	24.619	0.056	49.072	42.300	41.293	30.687	29.704	29
05/10/2018	467	27.549	0.083	47.429	45.549	47.733	34.923	32.953	59
06/10/2018	617	31.230	0.111	52.910	50.844	53.200	41.113	38.909	118
08/10/2018	563	31.712	0.139	61.284	41.481	42.607	38.147	37.076	102
09/10/2018	250	28.107	0.167	37.975	37.531	38.447	34.996	33.914	56
04/11/2018	415	22.499	0.056	42.021	40.274	42.439	27.748	25.928	34
05/11/2018	617	23.315	0.083	45.549	43.569	45.931	32.401	30.072	66
06/11/2018	447	22.969	0.111	42.042	40.779	42.497	34.494	32.535	64
07/11/2018	413	23.918	0.139	41.473	40.616	41.959	36.492	34.808	82
08/11/2018	554	23.807	0.167	42.709	41.150	43.170	34.970	32.775	119

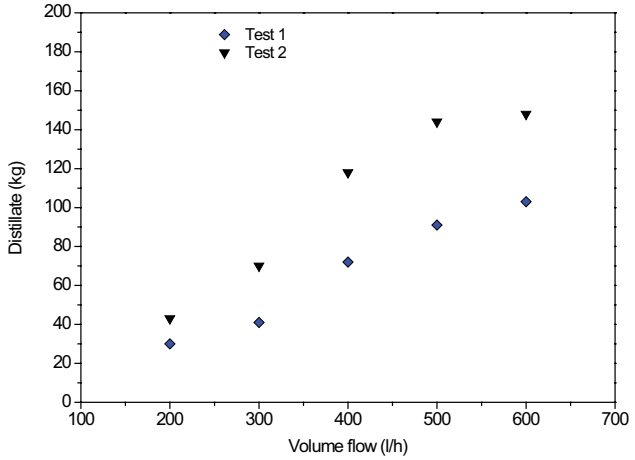

Fig. 11. Effect of feed volume flow on distillate.

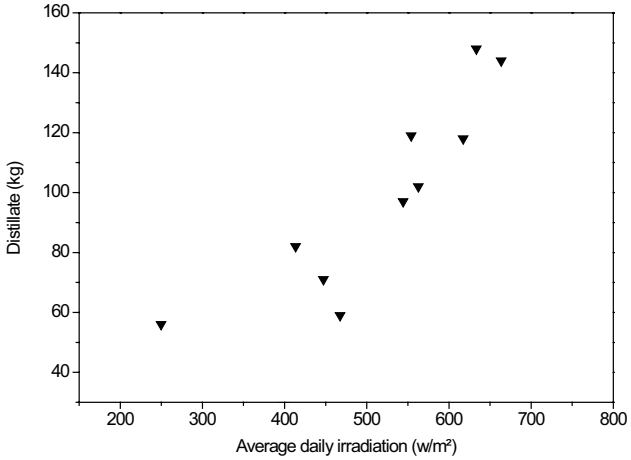

Fig. 12. Effect of solar irradiation on distillate.

volume flow is that a higher velocity causes less temperature polarisation at the feed side. Moreover, the difference in temperature across the membrane went up with rising feed volume flow, which brought about an exponentially increased difference in vapor pressure. Consequently, the distillate increased with increasing feed volume flow. The obtained result is experimentally confirmed by Winter et al. [16]. They inferred that, with increased volume flow, the temperature and concentration of the liquid–vapor interface get closer to that in the bulk, thus increasing distillate.

Fig. 12 shows the influence of solar intensity on distillate. In Fig. 12, it can be noticed that the distillate increases with the solar intensity at a constant volume flow of feed water (600 L h^{-1}). In fact, the increase in solar intensity increases the temperature of feed water. With the rise in feed water temperature, the partial vapor pressure rises on the feed side of the PGMD module. This, in turn, leads to a surge in driving force, which is the difference in water vapor pressure between evaporator and condenser channels, and hence mass transfer is increased.

4. Economic analysis

The major hurdle in water desalination processes driven by renewable energy sources is high initial investment costs; thus Payback period (Pb) and freshwater production cost (WPC) is chosen as the economic criteria for evaluating the efficiency of a solar water desalination system. In this section, the time period to recover initial investment cost is the basis for payback period calculation. The cost of each component constituting the experimental prototype obtained from suppliers in Tunisia and Germany is shown in Table 3. The cost of the water produced by the PGMD process depends on a large number of parameters. Generally, the evaluation method is based on the calculation of investment and operating costs. Thus, the total yearly cost

Table 3
Investment cost of each component constituting the experimental prototype

Prototype components	Quantity	Cost (€)	Total cost (€)
Photovoltaic module 245 W	4	188.5	754
Thermal solar collector 2 m²	3	214.6	643.8
Compact distillation module (PGMD, pumps, filters, feed tank and heat exchanger)	1	11,000	11,000
Piping/connection accessory	1	681.5	681.5
Circulation pump	1	101.5	101.5
DC pumping system	1	1,044	1,044
DC/AC protection box	1	275.5	275.5
Wiring and cable routing	1	217.5	217.5
Battery/charge regulator/inverter	1	788.8	788.8
Structure	1	174	174

of desalination, A_{tot}, is calculated as the sum of the yearly amortization or fixed charges, A_{fixed}, and the yearly maintenance and operating costs, $A_{O\&M}$:

$$A_{tot} = aA_{fixed} + A_{O\&M} \quad (1)$$

The amortization factor, a, is a function of the year or lifetime of the unit, n, and the yearly interest rate (%), i:

$$a = \frac{i(1+i)^n}{(1+i)^n - 1} \quad (2)$$

The unit price of produced water, WPC, is the ratio of the total yearly cost to the quantity produced yearly by the desalination unit:

$$\text{WPC} = \frac{A_{tot}}{f\dot{m}_{dis}365} \quad (3)$$

Since the desalination unit does not operate every day, a unit availability factor, f, has been introduced to adjust yearly expenditures. The economic study was conducted on the basis of a plant availability factor of 90%, a unit lifetime of 20 y and an interest rate of 5%. The land is offered by the University of Kairouan, Tunisia. Table 4 presents a summary of the cost evaluation results of the experimental prototype.

Table 4
Summary of the cost evaluation results of the experimental prototype

Capital cost	15,680.6 €
Operating and maintenance costs ($A_{O\&M}$)	250,886 € y^{-1}
Lifetime (n)	20 y
Interest rate (i)	5%
Amortization factor (a)	0.080 y^{-1}
Fixed charges (A_{fixed})	125,444 € y^{-1}
Total unit cost	150,533 € y^{-1}
Unit availability (f)	90%
Unit capacity	0.148 m^3 d^{-1}
Water production cost (WPC)	30.96 € m^{-3}
Net earning	30.95
Payback period (Pb)	506.60 d

5. Conclusions

This work presents the preliminary experimental results of a pilot operation with a 10 m² PGMD. The experimental set-up is totally autonomous; the only input power is solar radiation. The electrical energy required to run the pilot is ensured by a field of 4 modules of photovoltaic cells producing 1 kW. The required thermal energy to heat feed water is provided by a field of 3 flat-plate selective collectors offering a total surface of 6 m². Preliminary experimental tests conducted during six months demonstrate the behavior of the system in various weather conditions. The maximum freshwater production of 148 L d^{-1} was obtained on a sunny summer day in July of 633 W m^{-2} d^{-1}. In future works, the obtained freshwater production will be improved by integrating into the facility a storage tank, in order to extend the functioning of the facility at night. Then, the performance of PGMD will be compared with other MD configurations.

Acknowledgments

The authors are grateful to the Ministry of Higher Education, Scientific Research and Information and Communication Technologies MESRS-TIC for its financial support to the R&D project entitled "Solar-driven membrane distillation for resource-efficient desalination in remote areas". Thanks also go to the Fraunhofer Institute for Solar Energy Systems, ISE, for its collaboration.

Symbols

A	—	Annual cost, €
I	—	Solar radiation, W m^{-2}
T	—	Temperature, K
$\dot{m}$	—	Mass flow rate, Kg s^{-1}

Subscripts

amb	—	Ambiant
ci	—	Condenser inlet
co	—	Condenser outlet
dis	—	Distillate
ei	—	Evaporator inlet
eo	—	Evaporator outlet
sci	—	Solar collector inlet
sco	—	Solar collector outlet

Abbreviation

MD	—	Membrane distillation
MENA	—	Middle East and North Africa
MSF	—	Multi-stage flash
MED	—	Multi-effect distillation
RO	—	Reverse osmosis
VC	—	Vapour compression
V-MEMD	—	Vacuum-multi-effect membrane distillation
PTFE	—	Polytetrafluoroethylene
Pb	—	Payback period
WPC	—	Water production cost

References

[1] Y.Q. Wang, Z.L. Xu, N. Lior, H. Zeng, An experimental study of solar thermal vacuum membrane distillation desalination, Desal. Water Treat., 53 (2015) 887–897.
[2] J.H. Lienhard V, M.A. Antar, A. Bilton, J. Blanco, G. Zaragoza, Chapter 9 – Solar Desalination, In: Annual Review of Heat Transfer, Vol. 15, Begell House, Inc., New York, 2012, pp. 277–347.
[3] A. Essalhi, M. Khayet, Chapter 10 – Fundamentals of Membrane Distillation, A. Basile, A. Figoli, M. Khayet, Eds., Pervaporation, Vapour Permeation and Membrane Distillation: Principles and Applications, Elsevier (Imprint: Woodhead Publishing), ISBN: 9781782422464, 2015, pp. 277–316.
[4] S. Al-Obaidani, E. Curcio, F. Macedonio, G. Di Profio, H. Al-Hinai, E. Drioli, Potential of membrane distillation in seawater desalination: thermal efficiency, sensitivity study and cost estimation, J. Membr. Sci., 323 (2008) 85–98.
[5] K.W. Lawson, D.R. Lloyd, Membrane distillation, J. Membr. Sci., 124 (1997) 1–25.
[6] D. Winter, Membrane Distillation – A Thermodynamic, Technological and Economic Analysis, Dissertation at the University of Kaiserslautern 2014, Shaker Verlag, Aachen, 2015.
[7] J.A. Andrés-Mañas, A. Ruiz-Aguirre, F.G. Acién, G. Zaragoza, Assessment of a pilot system for seawater desalination based on vacuum multi-effect membrane distillation with enhanced heat recovery, Desalination, 443 (2018) 110–121.
[8] A.E. Kabeel, M. Abdelgaied, E.M.S. El-Said, Study of a solar-driven membrane distillation system: evaporative cooling effect on performance enhancement, Renewable Energy, 106 (2017) 192–200.
[9] A. Chafidz, E.D. Kerme, I. Wazeer, Y. Khalid, A. Ajbar, S.M. Al-Zahrani, Design and fabrication of a portable and hybrid solar-powered membrane distillation system, J. Cleaner Prod., 133 (2016) 631–647.
[10] H.E.S. Fath, S.M. Elsherbiny, A.A. Hassan, M. Rommel, M. Wieghaus, J. Koschikowski, M. Vatansever, PV and thermally driven small-scale, stand-alone solar desalination systems with very low maintenance needs, Desalination, 225 (2008) 58–69.
[11] A.S. Hassan, H.E.S. Fath, Review and assessment of the newly developed MD for desalination processes, Desal. Water Treat., 51 (2013) 574–585.
[12] F. Banat, N. Jwaied, M. Rommel, J. Koschikowski, M. Wieghaus, Desalination by a "compact SMADES" autonomous solar powered membrane distillation unit, Desalination, 217 (2007) 29–37.
[13] F. Banat, N. Jwaied, M. Rommel, J. Koschikowski, M. Wieghaus, Performance evaluation of the "large SMADES" autonomous desalination solar-driven membrane distillation plant in Aqaba, Jordan, Desalination, 217 (2007) 17–28.
[14] N.C. Barford, Experimental Measurements: Precision, Error and Truth, 2nd ed., John Wiley & Sons, New York, 1990.
[15] R.J. Moffat, Describing the uncertainties in experimental results, Exp. Therm Fluid Sci., 1 (1988) 3–17.
[16] D. Winter, J. Koschikowski, M. Wieghaus, Desalination using membrane distillation: experimental studies on full scale spiral wound modules, J. Membr. Sci., 375 (2011) 104–112.